

Real Time FRET Based Detection of Mechanical Stress in Cytoskeletal and Extracellular Matrix Proteins

FANJIE MENG,¹ THOMAS M. SUCHYNA,¹ ELENA LAZAKOVITCH,² RICHARD M. GRONOSTAJSKI,²
and FREDERICK SACHS¹

¹Department of Physiology and Biophysics, Center for Single Molecule Biophysics, State University of New York at Buffalo, 301 Cary Hall, Buffalo, NY 14214, USA; and ²Department of Biochemistry, Developmental Genomics Group, New York State Center of Excellence in Bioinformatics and Life Sciences, State University of New York at Buffalo, 119 Farber Hall, Buffalo, NY 14214, USA

(Received 18 May 2010; accepted 2 September 2010)

Associate Editor Yingxiao Peter Wang and Peter Butler oversaw the review of this article.

Abstract—A molecular force sensing cassette (stFRET) was incorporated into actinin, filamin, and spectrin in vascular endothelial cells (BAECs) and into collagen-19 in *Caenorhabditis elegans*. To estimate the stress sensitivity of stFRET in solution, we used DNA springs. A 60-mer loop of single stranded DNA was covalently linked to the external cysteines of the donor and acceptor. When the complementary DNA was added it formed double stranded DNA with higher persistence length, stretching the linker and substantially reducing FRET efficiency. The probe stFRET detected constitutive stress in all cytoskeletal proteins tested, and in migrating cells the stress was greater at the leading edge than the trailing edge. The stress in actinin, filamin and spectrin could be reduced by releasing focal attachments from the substrate with trypsin. Inhibitors of actin polymerization produced a modest increase in stress on the three proteins suggesting they are mechanically in parallel. Local shear stress applied to the cell with a perfusion pipette showed gradients of stress leading from the site of perfusion. Transgenic *C. elegans* labeled in collagen-19 produced a behaviorally and anatomically normal animal with constitutive stress in the cuticle. Stretching the worm visibly stretched the probe in collagen showing that we can trace the distribution of mean tissue stress in specific molecules. stFRET is a general purpose dynamic sensor of mechanical stress that can be expressed intracellularly and extracellularly in isolated proteins, cells, tissues, organs and animals.

Keywords—FRET, Stress, Cytoskeleton, Endothelial, *C. elegans*.

INTRODUCTION

There are three sources of energy for cells: chemical potential, electrical potential and mechanical potential. The first two have been well characterized but the third has not. Mechanical forces inside and outside of cells are pervasive, dynamic and distributed in three dimensions, but our understanding of these forces has been constrained by a lack of probes. Mechanical forces affect differentiation,^{2,16,25} tumor cell proliferation and apoptosis⁸ and cell locomotion. Most stresses in cells are born by the cytoskeleton where biochemistry and the physical forces of molecular crowding and stress sensitive bonds are inseparable.⁴⁶ With many cross-linked heterogeneous and anisotropic proteins, it is impossible to estimate internal stresses from macroscopic measurements. Single molecule force spectroscopy *in vitro* has shown that force applied to proteins produces distinctive changes in structure^{6,7,15,39} such as unfolding to expose cryptic sites that alter protein biochemistry.^{12,17,29} However, if one extends basic mechanics to molecular structure, we have to be able to translate the Poisson constant, for example, to compression in a stretched subcellular fiber (see “**Discussion**” section). To investigate the *in vivo* distribution of molecular stress in space and time we constructed a FRET based stress probe that could be expressed in specific proteins in living cells and animals.²⁸

The probe called stFRET consists of green fluorescence protein mutants (Cerulean as the donor and Venus as the acceptor^{32,38}) linked by a stable 5 nm alpha-helix whose linear length is the characteristic Forster distance for the FRET pair (if one assumes random tumbling), and the most sensitive operating point for sensing strain. Our initial study characterized the probe and showed that it can be efficiently

Address correspondence to Thomas M. Suchyna, Department of Physiology and Biophysics, Center for Single Molecule Biophysics, State University of New York at Buffalo, 301 Cary Hall, Buffalo, NY 14214, USA. Electronic mail: suchyna@buffalo.edu, rgron@buffalo.edu

F. Meng and T. M. Suchyna are co-first authors.

incorporated into structural proteins such as collagen-19, non-erythrocyte spectrin, α -actinin and filamin A without disrupting their normal distribution.²⁸

Spectrin, α -actinin and filamin A are actin cross-linking proteins that are known to participate in signaling pathways and can be unfolded or separated from their partners at physiological levels of stress.^{11,13,42,43} The spectrin repeat in spectrin and actinin melts at 40–45 °C, close to homeotherm body temperatures, so the “equilibrium” structure is predicted to have large deviations with obvious relevance to spectrin and actinin pathophysiology.^{24,51} *In vitro* mechanics studies of spectrin family proteins have shown that the force-distance curve of helices has three phases: a linear Hooke’s domain of about 10 pN/nm, a relatively flat region where the helix repeats unfold independently at much lower forces (25–35 pN) than beta sheet proteins, and a wormlike chain (WLC) region at higher forces.³⁷ How the molecular forces relate to the mean macroscopic forces was illustrated in a recent report showing that fluid shear stress can expose cryptic cysteines in spectrin within living cells.¹⁷

Filamin A is a cytoskeleton protein that crosslinks orthogonal actin filaments^{9,33} and thus reinforcing the cell cortex.^{9,18} Atomic force microscopy (AFM) data of the filamin A IgG-fold domain shows that it reversibly unfolds with large forces, 50–220 pN.¹³ However, the binding of actinin and filamin to actin, which have homologous actin binding domains, can rupture at similar forces (40–80 pN).¹¹

We genetically incorporated stFRET into a variety of cytoskeletal proteins in BAECs using acute transfection with chimeric constructs. To observe stresses in living animals *in situ*, we labeled collagen-19⁴⁵ in *Caenorhabditis elegans*. The cuticle is composed of crosslinked collagens and other proteins in a highly structured extra-cellular matrix that is the attachment structure for the body muscles and maintains tissue morphology.^{19,20} With stFRET probes in transgenic animals we could observe spatially varying constitutive strains that could be modified with external stress. Thus *in vitro* and *in vivo* data demonstrate that stFRET has sufficiently sensitivity to probe mechanical stresses in real time in living cells, tissues and animals and that there are gradients of stress that differ among crosslinking proteins and need not correspond to obvious histological markers of cell shape.

RESULTS

Robust Energy Transfer of stFRET and Its Sensitivity to Forces In Vitro

A FRET pair has maximal sensitivity to axial strain when the distance between the donor and acceptor is

R_0 .^{32,38} Since the FRET probe always has a 1:1 stoichiometry of donor to acceptor, we utilized the FRET ratio as a measure of probe strain and host stress. The FRET ratio is affected by the length of the linker and angle between the fluorophore dipoles, both of which can be altered by stress in the host protein. These changes are reversible.³⁷

The force sensitivity of stFRET was assessed *in vitro* using DNA springs as mechanical stimuli as illustrated in Fig. 1a. A 60-mer of single stranded (ss) DNA (> 20 nm in unfolded length) was covalently linked to the cysteines at positions 48 of both donor and acceptor. Since ssDNA is a floppy polymer with a short (1 nm) persistence length it doesn’t apply much force to the stFRET probe which if extended would have an end to end distance of ~13 nm. However, double stranded (ds) DNA is much stiffer. Addition of complementary DNA that anneals to the 60-mer ssDNA (with a persistence length of 50 nm) corresponds to a 10–20 kT increase in free energy⁴⁹ that acts to stretch stFRET. For reference, the thermodynamic (melting) stability of a 100 amino acid protein is on the order of 10–20 kT.³⁵ Force from the DNA could be released either by digestion with nuclease or cutting the dsDNA with *EcoRI*. Agarose gels clearly showed the binding of the DNA to protein (Fig. 1b) since under UV illumination, purified stFRET protein is green while ethidium bromide stained DNA is orange. The DNA–protein complex emits yellow light and, as expected, the migration of the bound DNA was retarded.

stFRET has a strong emission peak at 525 nm with emission of the donor at 475 nm, a spectrum similar to an equimolar mixture of monomeric Cerulean and Venus (Fig. 1c). Compared to pure stFRET protein in solution, the ssDNA linked protein showed a decreased FRET ratio: 2.7–1.7, and decreased donor quenching: 0.3–0.6 (Fig. 1d). This result suggests that even ssDNA can apply some extension force to stFRET, probably as an entropy spring that happens to move the fluorophores to less favorable angles. However, after introducing complementary DNA, the FRET ratio dropped to ~1 and the donor emission recovered to 0.8. For comparison, dilute equimolar Cerulean and Venus monomers in solution have a FRET ratio of ~0.3.²⁸ Five minutes of nuclease digestion of the bound DNA at room temperature restored the FRET efficiency of stFRET to that of the unliganded protein. Similar behavior occurred after dsDNA was digested by *EcoRI*. Nuclease and *EcoRI* alone had no effect on native stFRET protein fluorescence (Figs. 1c, 1d).

stFRET Detects Constitutive Strain in Cytoskeletal Proteins

We incorporated stFRET into three cytoskeletal proteins (actinin, spectrin and filamin) that are known

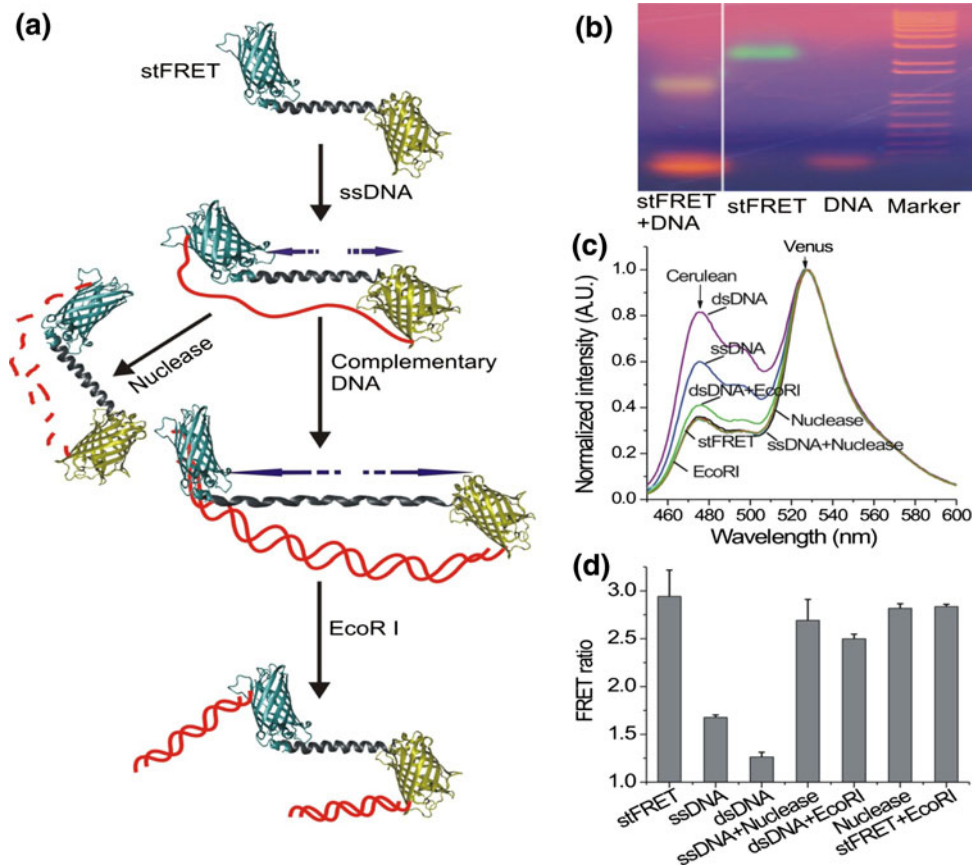


FIGURE 1. The relationship between the FRET ratio and linker strain (S). stFRET was stretched *in vitro* with ss and ds-DNA as illustrated in (a), where $S = 0$ at R_0 . The stFRET cassette was stretched using a DNA spring attached to the two fluorophores (cyan, Cerulean; yellow, Venus; gray, alpha-helix; orange, ssDNA). Stress was increased by the addition of complementary DNA forming a distended dsDNA loop which was then released by enzymatic cleavage of the DNA. (b) Electrophoretic separation of the reaction mixture of stFRET protein (green), DNA stained with ethidium bromide (red), and the DNA-stFRET complex (yellow). (c) Spectra of the DNA-stFRET complex and free stFRET with different DNA linkers and treatments that affect the stress are labeled. Excitation was set at 433 nm. (d) Calculated FRET ratio of DNA-stFRET complex and stFRET under different treatments.

to bundle actin fibers. stFRET was inserted at the locations shown in Figs. 2a–2c. We have found that probe locations near the middle of the host and away from known sites of interaction tends to leave the protein distribution unaltered.²⁸

The FRET ratio dynamic range needs to be calibrated for each optical system because of differences in the optics and notably the filters. The dynamic range of the FRET ratio in the microscope was determined using the isolated stFRET protein in solution and then cleaving the linker with trypsin (that does not affect the fluorophores²⁸) to approximate the maximum and minimum values (Fig. 2d). The ratio ranged from 5.5 for the intact probe to 0.5 for the cleaved one. We obtained another estimate of the minimum FRET value by coexpressing Cerulean and Venus monomers in BAECs at a 1:1 DNA ratio at concentrations that corresponded to effectively infinite separation, and we obtained a mean ratio of 0.5. Surprisingly, the monomers showed some nuclear accumulation, but the FRET ratios (averaging <1),

remained spatially invariant showing the *in vivo* results were not concentration dependent (Fig. 2e).

All three cytoskeleton proteins reported spatial variations in FRET often localized to specific subcellular domains (Figs. 2a, 2c). The mean FRET ratios, averaged across each cell, had constitutive values of 1–3 (Fig. 2d). Spectrin had the lowest ratio (highest constitutive stress) and also showed punctuate patterns throughout the cell (supporting Fig. S1). In contrast, actinin and filamin localized along actin tracks. We tested the strength of binding to actin by solubilizing the cell with TritonX-100 that leaves much of the cytoskeleton intact creating “cell ghosts”. Consistent with a tight actin association of actinin and filamin, these proteins remained in the ghosts but the more loosely bound spectrin washed away. In ghosts, actinin and filamin retained the stressed FRET ratio of untreated cells. We observed consistent spatial variations in local stress. For example, the perinuclear region displayed lower FRET ratios corresponding to

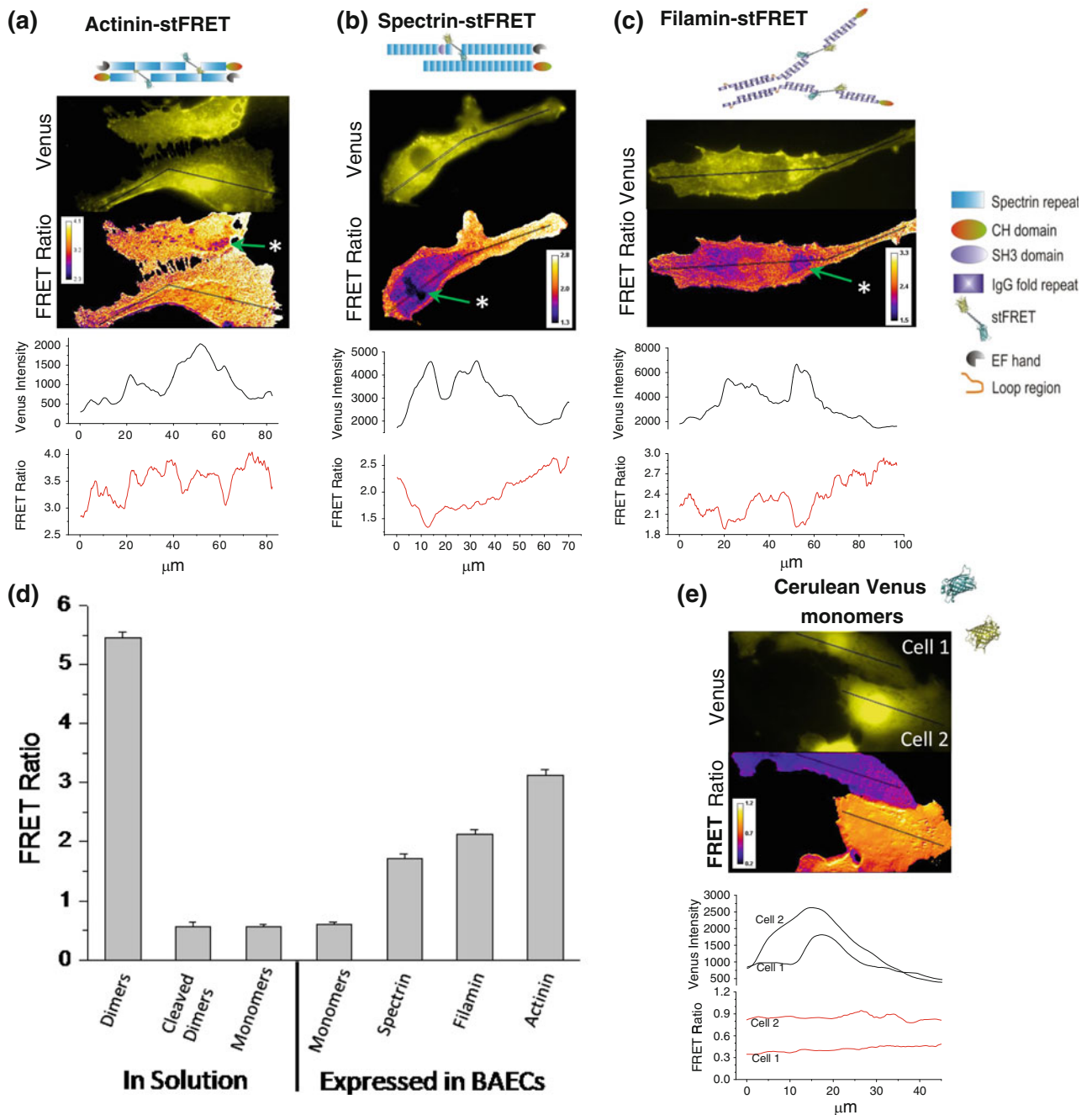


FIGURE 2. stFRET constructs detect constitutive strain in living cells. (a–c) Each panel shows an illustration of the expressed protein in BAECs at the top, a Venus and a FRET ratio image of representative cell(s) and line profiles graphs from the black lines going through both images. (a–c) Cartoons show stFRET insertion points; spectrin between spectrin repeat domain 8 and 9, actinin between spectrin repeats 1 and 2 and filamin between IgG-fold domains 8 and 9. A protein domain key is shown to the left. Each image shows migrating subconfluent cells with thin tails at the trailing cell region. An asterisk indicates perinuclear regions with lower FRET ratios. (d) Average FRET ratios observed with Zeiss AxioObserver for stFRET dimers ($n = 1$), stFRET cleaved with trypsin ($n = 7$) and Cerulean and Venus monomers ($n = 7$) in solution. Corresponding measurements of the free Cerulean and Venus monomers ($n = 20$) spectrin ($n = 12$), filamin ($n = 9$) and actinin ($n = 15$) stFRET constructs expressed in BAECs show intermediate constitutive FRET ratios. (e) Control cells expressing Cerulean and Venus monomers show significant variation in the distribution of protein intensity but little variation in FRET intensities. Difference in average FRET ratio between cell 1 and 2 are due to stochastic differences in the ratio of DNA vectors transfected into each cell.

higher stress (“*” in Figs. 2a–2c—probably endoplasmic reticulum and Golgi). In subconfluent cultures with migrating cells, filamin and spectrin showed

gradients of stress with higher stress (lower FRET) toward the leading edge and lower stress toward the lagging side consistent with observations in fibroblasts.²⁸

As expected, internal tension decreased with decreased adhesion of the cells to the substrate. Rounded cells separating from the substrate showed relatively uniform protein distribution and FRET ratios (Fig. 3a, detached) while adherent cells show a mosaic of stress gradients (Fig. 3a, attached). The spontaneously rounded cells may have been undergoing mitosis and we are currently examining how stresses vary during cell division. In fully detached cells, the FRET ratio was significantly higher (less tension) in all three proteins (Fig. 3b). To test whether adhesion itself was necessary for creating internal stress, we deliberately loosened the cells from the coverslip with dilute trypsin (Fig. 3a, trypsinized). All three constructs showed increased FRET ratios, with filamin being the most strongly affected, and the protein distribution throughout the cell became uniform. To explore the role of f-actin we disrupted it with actin inhibitors expecting that this would relieve stress on the three proteins. However, the FRET ratio for all three proteins rapidly decreased by 6–8% (Fig. 3c) suggesting that the labeled proteins are mechanically not in series with actin and probably have a normal component.

Since cell adherence to the substrate effects cell shape we monitored the lateral cell area at the level of the coverslip (Fig. S2). Even in the absence of drugs, cells showed a weak contraction over the first hour upon removal from the incubator and placed in normal saline at RT. When exposed to actin inhibitors, the cells did not round up like the trypsinized cells (videos in Figs. S2A–S2C), though actinin labeled cells showed a bit more sensitivity than controls of filamin and spectrin labeled cells (Fig. S2D). Cells washed with new saline at this time point were completely unaffected, and cells treated with saline plus 2.5% DMSO (vehicle) produced a very small 1.5% decrease. Again, this shows that the cytoskeleton is heterogeneous in both structure and mechanics.

Dynamic FRET During Acute Mechanical Stimulation of BAECs

We applied 500 ms pulses of shear stress from a micron diameter pipette driven with a pressure clamp⁴ (Fig. 4 and supporting Video S3). From numerical simulations (COMSOL software) we estimated the shear force to be 20–40 dyn/cm², similar to *in vivo* shear stresses experienced by endothelial cells. All constructs showed sensitivity to shear, but the FRET changes were variable in intensity and time (see “Discussion” section) and hence hard to quantify. Figure 4a shows a “typical” result from a spectrin labeled cell where we perfused orthogonally to a narrow region of a cell. We measured the FRET ratio in four regions of interest (ROI) from the upstream to the

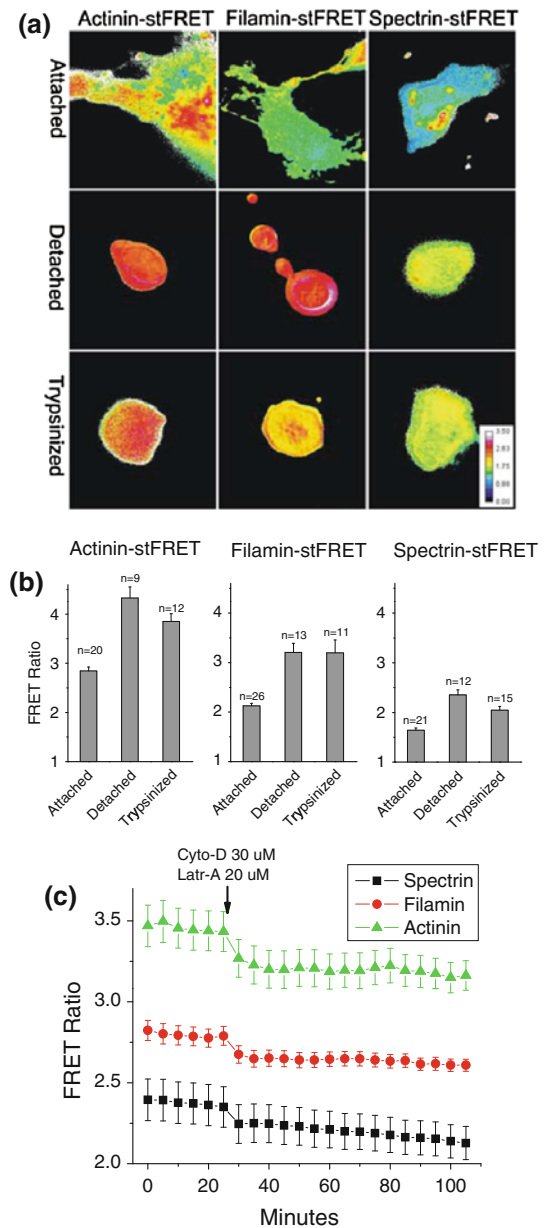


FIGURE 3. Strain on cytoskeleton proteins in different cellular conformations. (a) FRET ratio images of actinin, filamin and, spectrin stFRET constructs expressed in BAECs when attached, naturally rounded up and detached by trypsin (scale bar = 5 μm). (b) Bar graphs show the average FRET ratio for each treatment group. (c) Average FRET ratios shown over time from BAECs expressing spectrin ($n = 25$), filamin ($n = 21$) and actinin ($n = 16$) stFRET. At 25 min cells were treated with 30 μM Cytochalasin D and 20 μM Latrunculin A. All cell types showed a modest FRET decrease (spectrin 7%; filamin 6%; actinin 8%).

downstream side of the cell as it flexed under the flow. Using an ImageJ macro the ROIs dynamically tracked the motion of the upstream and the downstream edges of the cell. In all ROIs the FRET ratio decreased with shear stress suggesting an increase in local tension, but

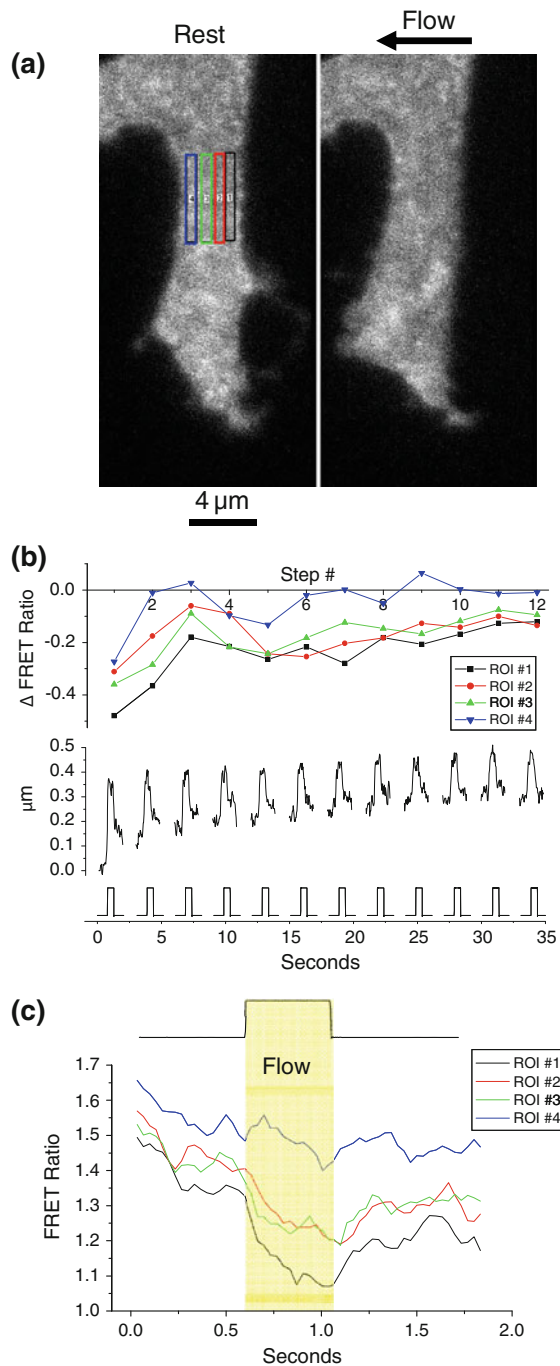


FIGURE 4. stFRET is sensitive to mechanical stimulation. (a) Venus image of a region of a BAEC cell expressing spectrin stFRET showing the cell before the flow and while being deformed by fluid shear stress from a pipette positioned about 20 μm to the right. Four color-coded ROIs are arranged from the upstream side to the downstream side of the cell. (b) shows the change in the FRET ratio at the different ROIs (ΔFRET ratio) and the motion of the cell's leading edge for each fluid shear pulse which are shown at the bottom. The magnitude of the motion and the ΔFRET ratio decreased rapidly in unison over the first four pressure steps. (c) Real time average (averaged pulses 1–12) FRET ratio measurements for the four ROIs shows that under shear stress there is a graded FRET decrease from the upstream to the downstream side.

the magnitude depended on the position of the probe with respect to the direction of flow. Repeated shear pulses showed a slow (5–10 s) adaptation in all ROIs with more tension at the upstream side and less at the downstream side for both single sweeps (Fig. 4b) and the averaged response (Fig. 4c). This adaptation corresponded to significant cell stiffening with the cell movement decreasing for the same shear stress (Fig. 4b). In the ROI at the leading edge, the first shear pulse produced a relatively large $\sim 50\%$ decrease in the FRET ratio (black trace Fig. 4b) that attenuated to $\sim 20\%$ by step number 12. At the trailing edge there was an initial 25% decrease that attenuated to $< 5\%$. (This attenuation was too rapid to be caused by photobleaching, $\tau_{\text{Venus}} = \sim 60$ s, see Fig. S4.)

stFRET Reveals Collagen Stress in Response to External Stress in Living C. elegans

Transgenic worm lines were developed expressing stFRET inserted into collagen-19 at three positions (C1–C3) as illustrated in Fig. 5a. We tested the effects of transfection by starting with collagen terminally tagged with GFP. This showed the common striated fluorescence distribution pattern and three central seam lines along the alae (Fig. 5b, panel collagen-GFP). We observed a similar collagen distribution pattern only in worm line C3 (Fig. 5b) where stFRET was incorporated between two Gly-X-Y domain and in front of second cysteine cluster domain. Apparently, the other two locations affected the targeting and assembly of collagen-19 although it clearly was nonfatal. Constitutive stresses were apparent, but it was hard to make the measurement in moving worms especially in structures only a few microns wide such as the annuli rings. To obtain better images of the collagen distribution in the cuticle C3 worms were solubilized with detergent using three separate techniques (supporting Fig. S5). SDS detergent formed the cleanest preparation and we could see stress that varied with location especially about the annuli, alae and mouth (supporting Fig. S6). The largest variations in constitutive stress were observed near the mouth, and along the annuli where we observed a ribbed pattern in the FRET ratio. Stress is clearly not homogenous within specific locations at the light microscope resolution.

Live transgenic worms in the microscope moved rapidly to avoid the illumination making it difficult to analyze the dynamic changes in stress. To immobilize the worm we held it with two suction pipette positioned with manipulators and focused the microscope on the portion of the worm held by a fixed manipulator. We observed significant constitutive strain in the cuticle at the constricted region near the pipette tip due to compression. To observe the effects of external

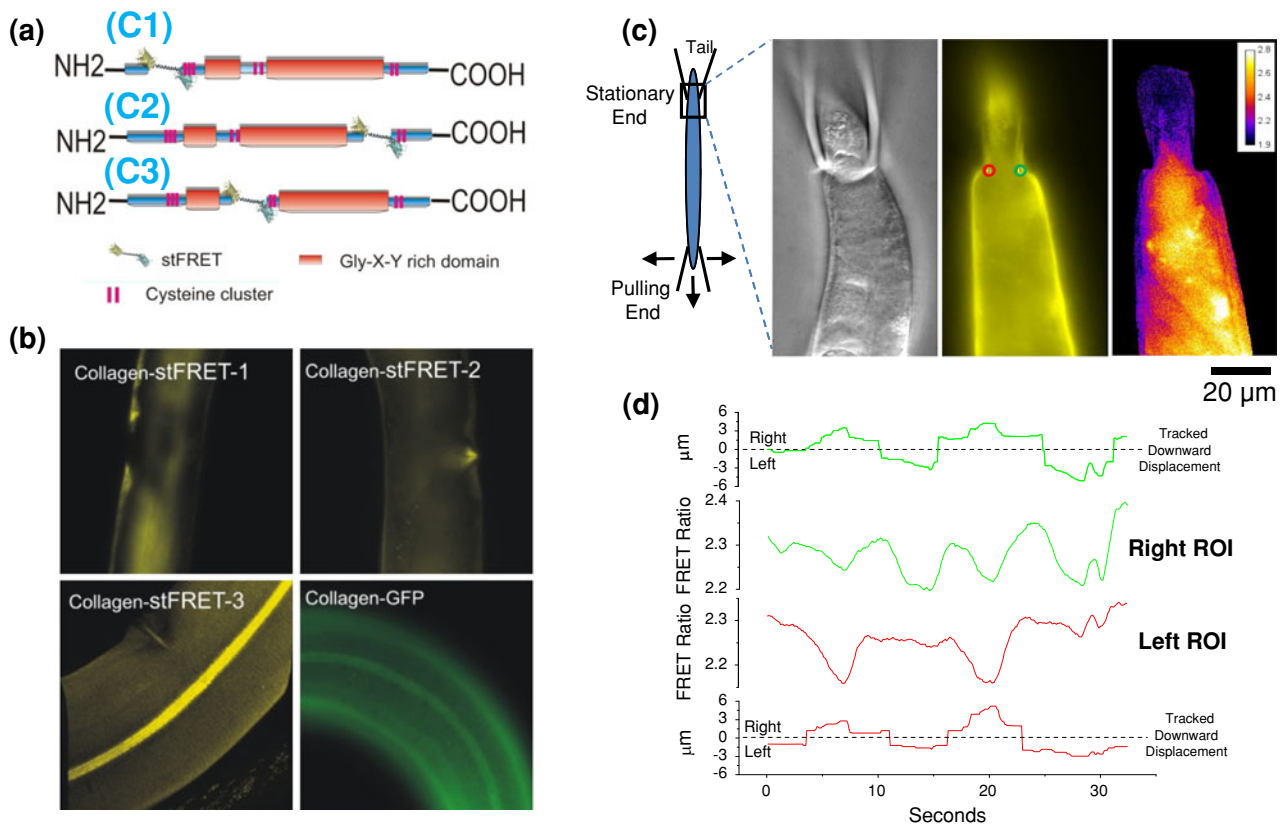


FIGURE 5. Localization and strain in collagen-19-stFRET expressed in live *C. elegans*. (a) Domains and locations of stFRET probes are illustrated in three collagen-19 constructs labeled C1, C2 and C3 as per methods. (b) Fluorescent images of the three different stFRET collagen constructs and a C-terminal EGFP tagged collagen-19 as a control. C3 is the only stFRET construct that shows the same distribution as the EGFP construct. (c) Two micropipettes were used to restrain a stFRET transfected worm for imaging during stretch. This allowed stretching the worm with the bottom pipette while maintaining focus on the stationary pipette. The monitored region is shown in expanded panels to the right with DIC, Venus and FRET ratio images. The tail of the worm is being held by the stationary pipette in this image. Two ROIs are shown imposed on the Venus image to the right (green) and left (red) of the pipette opening where we expected the greatest strains. (d) Shows colored coded graphs of the displacement of right and left ROIs and the corresponding FRET ratio. The displacement graphs show downward motion that shifts across the dotted baseline line from right to left depending on the movement of the pipette tip.

stress on collagen-19, we pulled the other end of the worm with a mobile manipulator (Fig. 5c). To quantify the effect we placed two ROIs on either side of the worm near the fixed pipette restriction and pulled the worm down and sideways parallel to the chamber bottom (supporting Video S7 shows the dynamic response). We tracked the edge of the worm using mobile ROIs as described above. Figure 5d shows that both ROIs had a significant decrease in the FRET ratio with stretch (increased tension in collagen). The responses on the two sides were asymmetric due to asymmetries in the worm, the opening of the fixed pipette tip shape and the pulling motions (Fig. 5c).

DISCUSSION

Our attempts to obtain a rough force calibration of the probe using DNA springs were successful in that

we could readily resolve the forces due to a change in persistence length. What is that force? The experiments and analysis by Zocchia's group suggest that they are in the range of 5–7 pN.³⁶ When the bending of the DNA is relatively small, it can be well approximated by the mechanics of bending an elastic rod. However, stress from high curvature at length scales below the accepted persistence length for ds-DNA, can cause a kink in the DNA to form and thus limits the force.^{36,50} There is no force/distance data available for the linker that we used, but single molecule force spectroscopy of helices from spectrin³⁷ and myosin⁴¹ show a constant compliance up to ~40 pN. More precise calibrations of stFRET will require varying the length of the ss and complementary DNA and a better theory of DNA bending at these short length scales. Zocchi's group has shown that stresses seem to be distributed over the host protein,⁴⁸ but we should point out that the DNA is not attached at the C and N termini where the host protein

is attached, but at the cysteines of GFPs. These different geometries could produce somewhat different values of R_0 due to the geometric factor of κ^2 .²⁸

However, the primary utility of these probes is to measure gradients of stress at the resolution of the light microscope, so that this means averaging the effects over a voxel volume. This will include many molecules that could be at different regions of the force distance curve,³⁷ fibers containing bilabeled peptides, monolabeled peptides or unlabeled peptides that are in parallel with the labeled ones since we did not suppress the endogenous gene expression. The data could also include crosslinkers that dissociated from actin and are averaged over the exposure time and over the voxel volume. Molecular erythroid spectrin tetramers can dissociate under shear stress at their dimer-dimer interaction ends.¹ Filamin binding to actin can be ruptured at forces similar to the stress required to unfold its Ig-like subdomains.¹¹ The adaptation effects we observed with repetitive shear stress with BAECs were possibly due to reforming of the cytoskeleton with new links, stabilization of some existing links, or both. But to visualize stress gradients at optical resolution, we do not need to know the absolute stress on a given molecule. In the long run, making a more homogenous population by suppressing expression of the wild type gene with iRNAs could lead to an improved signal to noise ratio.

The proteins we have chosen to label are hopefully representative of the fibrous proteins in and around cells. Actinin and filamin are actin bundling agents that are recruited to focal adhesion complexes and stress fibers. While actinin primarily acts to crosslink fibers that run in parallel longitudinally in stress fibers, filamin appears to crosslink actin fibers that are crossing.^{11,14} Spectrin is a crosslinking protein that primarily resides in the cortical cytoskeleton and acts as a scaffolding protein for membrane complexes, e.g., it links cell-cell junctions to perijunctional actin band in endothelial cells.³ Collagen is the most common protein in animals²² and our successful expression of an extracellular protein with the stFRET probe suggests that it, and related probes, will be extremely useful in understanding the mechanical function of the extracellular matrix and the glycocalyx.

We found that stFRET was least disruptive to normal protein distributions of all four host proteins when positioned centrally in the host. Collagen-19 was especially sensitive possibly due to the two cysteine clusters located at the C and N-terminals that form disulfide bridges between collagen monomers in the extracellular matrix.³⁰ All four protein constructs had constitutive FRET values within the dynamic range determined from the free stFRET probe in solution (pulled tightly together by the linker) and the cleaved

dimers (effectively infinitely apart). The distribution of FRET values within a single cell or organism differed by as much as 50% showing the presence of constitutive spatial and temporal stress gradients, features that are not currently visible through cell morphology. Since most filamentous proteins cannot be compressed due to buckling, prestressing these elements reflects not only mechanical reinforcement but provides for high speed (m/s) signal processing since viscosity effects are minimized.³¹ The detergent solubilization of worm cuticles showed that there is constitutive stress even in these nonliving demembrated preparations (supporting Fig. S6).

Much of the internal stresses in cells are reaction forces applied to adhesion plaques. These constitutive stresses could be mostly relieved by detachment of the cell from the substrate as evidenced by the rather uniform FRET in rounded cells. Stress applied to the plaques is generated mostly by actin and is sensitive to actin reagents,⁴⁷ however our data shows that the crosslinking proteins showed a modest but rapid *increase* in stress with the actin inhibitors. The stress increase could have several origins. The actin reagents are effective only on cycling actin²¹ and cortical actin has a slow turnover²³ so that release of stress for deeper actin and other linked cytoskeletal proteins would be transferred to the cell cortex that is still intact. Furthermore, actinin and filamin will produce tension in an actin network simply from crosslinking^{10,40} which again could be redistributed upon treatment with actin inhibitors. Also, some actin assembly is known to occur in the presence of latrunculin due to resistant actin oligomers.³⁴ In this regard, we noted that that while treated cells showed an overall decrease in contact area with the glass, there were still incidences of filipodial extension (see actinin video in Fig. S2C). Finally, if the regions of crosslinker binding are not broken down, the Poisson effect (stretched things getting thinner) will tend to stretch cross linkers as tension is removed in the primary filaments.

Mechanically induced strains from fluid shear on BAECs showed that the stFRET can dynamically report gradients of stress distributed differently over complex cell shapes. Quantitative analysis of these stresses remains a difficult analysis problem, but in our first order analysis of the initial shear pulse we saw a >50% increase in tension at the upstream edge and ~20% increase at the downstream side. The FRET response was viscoelastic (time dependent) and showed slow adaptation as expected for cytoskeletal networks^{26,44} that correlated with changes in cell stiffness.

The experiments on *C. elegans* showed that stFRET can be used to examine micromechanics *in situ*. We have begun extending these transgenic studies to mice where insertion of the labeled actinin has no effect on

behavior or development or reproduction. These preparations will allow us to study the stress in different organs and tissues such as the heart and bone in a variety of normal and pathological states. As we have shown, we can detect internal stress in specific proteins from the application of external stresses to the animal with a time resolution <10 ms.

stFRET is providing data on processes that were heretofore invisible. How can the probe be improved? An ideal probe would have the compliance of the host protein so that the physical behavior of the host is not compromised. We have done this recently by replacing the α -helix linker in stFRET with the spectrin repeat. Ideally we would like a higher contrast probe. However, for linkers with a linear compliance, the effective contrast with stress is limited by thermal energy that will cause the probe to change conformation in the same manner as an applied force. If the probe is operating in a nonlinear portion of the force-distance relationship as occurs with single molecule unfolding, we should be able to increase contrast at the expense of sacrificing linearity. And finally, as with nearly all fluorescent probes, increased photostability is a persistent and unmet goal.

MATERIALS AND METHODS

Gene Construction and Protein Purification

pEYFP-C1 Venus and pECFP-C1 Cerulean plasmids are generous gifts from Dr. David W. Piston.³⁸ stFRET gene construction is as described in our previous publication.²⁸ To purify the protein, stFRET gene was sub-cloned into prokaryotic expression vector pET-52b(+) (Novagen, Gibbstown, NJ, USA) using *Bam*HI and *Not*I restriction sites which were introduced into stFRET DNA fragment by primers: 5'-GCTTCAGCTGGGATCCGGTGGTATGGTGAGCAAGG-3'; 5'-CCAGATCGCGGCCGCTTAGTGGT GATGATGGTGGTATGATGCTTGTACAGCTCGTCC-3'. Following 8-histidine tag TAA stop codon was inserted in front of *Not*I site to make sure that His-tag located in C-terminal and well-exposed to solution.

To create chimeric gene constructs of filamin A, alpha actinin, non-erythrocytic spectrin and collagen, we subcloned collagen gene into Pinpoint Xa-3 vector and filamin, actinin, spectrin genes into pEYFP-C1 vector where YFP gene was removed beforehand. The followings are primers used and restriction enzyme sites introduced into PCR products for subcloning: Collagen, sense, 5'-CAGCTTGGCTGCAGCATTTGAAAATTTGCACCAATG-3' with *Pst*I, anti-sense 5'-AGTGCACCATATGCAGTACCCCTCATATCACTC-3' with *Nde*I; Actinin, sense, 5'-CAGATCCGC TAGCATGGACCATTATGATTCTCAGCAAACC-3'

with *Nhe*I, anti-sense, 5'-GATCCCGGGCCCCGCGGTACCTTAGAGGTCACTCTCGCCGTAC-3' with *Kpn*I; Filamin A, sense, 5'-GTGTATCATATGCCAAGTACGCCCCCTATTGACG-3' with *Nhe*I, anti-sense, 5'-GAAGCTTGAGCTCTTAGGGCACCACAACGC-3' with *Sac*I; Spectrin, sense, 5'-GCTAGCGCTACCGGTATGGACCCAAGTGGGG-3' with *Age*I, anti-sense, 5'-GGGCCCCGCGGTACCGTTCACGAA AAGCGAGC-3' with *Kpn*I. stFRET were inserted at three locations on collagen: 1, N-terminal at amino acid position 9 by *Bam*HI and *Not*I restriction sites; 2, C-terminal at position 131 by *Hind*III and *Not*I; 3, In the middle of collagen, position 71 by *Hind*III and *Not*I. Actinin was targeted by stFRET at position 300 with *Age*I and *Not*I, between spectrin repeat domain one and two. Spectrin was targeted at position 1300 between spectrin repeat domain eleven and twelve with *Sac*II and *Not*I. Filamin hosted stFRET at position 1000, between IgG fold domain eight and nine with *Age*I and *Not*I. All restriction enzyme sites were introduced into the host proteins by site-directed mutagenesis kit from Stratagene (La Jolla, CA, USA) with the original amino acids unchanged. Corresponding restriction sites for stFRET insertion were added by PCR. All chimeric construct sequences were confirmed by sequencing at Roswell-Park Cancer institute (Buffalo, NY, USA).

Protein-DNA Complex Synthesis and In Vitro DNA Stretching

A 60-mer DNA, [AminoC6]GAGTGTGGAGCC TAGACCGTGAATTCCTGGCAGTGGTGCGACC GACGTGGAGCCTCCCTC[AmC7Q], and the complementary strand were purchased from Operon (Huntsville, AL, USA). The oligo had amino modifications on both ends and an *Eco*RI cleavage site was introduced in the middle of the sequence that was selected from a previously study.⁴⁹ Fifteen nmol of DNA were incubated with 300 nmol heterobifunctional crosslinker SMPB (succinimidyl 4-[*p*-maleimidophenyl] butyrate) (Pierce, Rockford, IL) in 20 μ L conjugation buffer (100 mM sodium phosphate, 150 mM NaCl and 1 mM EDTA at PH 7.5) for 2 h at room temperature. The amino groups of the DNA reacted with the NHS-ester group of the crosslinker. The reaction mixture was passed twice through protein desalting spin columns (Pierce, Rockford, IL) to remove excess uncoupled crosslinkers. The DNA-crosslinker construct was then incubated with 1.5 nanomol purified stFRET protein in conjugation buffer with total volume 50 μ L. The donor and acceptor of stFRET have two free sulfhydryls from cysteines 48 and 70. The 70 position is inside the β -barrel and thus inaccessible, and the 48 position is only partially exposed to solution. To

accelerate the reaction of the maleimides with the DNA-crosslinker construct at sulfhydryls at the 48 position, we incubated the mixture at 37 °C for 30 min. Since DNA does not interfere with the FRET measurements, no further purification was necessary. To stretch stFRET, fifteen nanomols of complementary DNA were added to the protein-single strand DNA complex. The solution was left at room temperature overnight to complete the annealing. FRET measurements with the different DNAs attached were performed with a fluorescence spectrometer (Aminco-Bowman® series 2 luminescence spectrometer). We have used the FRET ratio as the energy transfer index: $\text{FRET Ratio} = (I_A - I_{\text{Dbt}})/I_D$, where I_A is the peak acceptor emission signal of stFRET, I_D is the peak donor emission signal and I_{Dbt} is the signal in the acceptor channel due to donor signal bleed-through.

FRET Ratio Calculation and In Vitro Measurements

For the DNA stretching FRET measurements we used a fluorescence spectrometer (Aminco-Bowman® series 2 luminescence spectrometer). All purified proteins were exchanged into 10 mM Tris-HCl buffer before further processing. The measurement was performed at room temperature with 200 μL of 10 μM protein. The spectrometer was set to: 4 nm bandpass, 1 nm step size, and 450–550 nm emission scan range for stFRET. Excitation wavelength was set at 433 nm. We have used the FRET ratio as the energy transfer index: $\text{FRET Ratio} = (I_A - I_{\text{Dbt}})/I_D$, where I_A is the peak acceptor emission signal of stFRET, I_D is the peak donor emission signal and I_{Dbt} is the signal in the acceptor channel due to donor signal bleed-through. All signals were recorded with 433 nm excitation. Because peak values from the spectrograms were used, the ratios are not directly comparable to the ratios obtained from the microscope.

Cell Culture Transfection and C. elegans DNA Transformation

BAEC cells were cultured in Dulbecco's Modified Eagle Medium (GIBCO® Invitrogen, Carlsbad, CA, USA) supplemented with 10% fetal bovine serum and antibiotics. Cells were spread on 35 mm coverslips and allowed to grow for 24 h. Fugene 6 (Roche) was used to deliver 2.0 $\mu\text{g}/\text{coverslip}$ of plasmid DNA to the cells. 24–36 h after transfection, the cells displaying moderate fluorescence were selected for observation. Highly expressing cells were avoided as they often showed bright spots that were apparently aggregates. The *C. elegans* germline transformations were performed as previously described.²⁷ Strain pha-1 was maintained at 15 °C. Chimeric collagen-stFRET

constructs were mixed with rescue plasmid (PBX-1) 1:1, 25 ng/ μL , and injected into worm gonads by a standard microinjection procedure.²⁷ Recovered worms were transferred to new dishes at 15 °C for 24 h, then F1 progenies were transferred to 25 °C for selection. After the surviving worms became adults, they were screened under a fluorescence microscope and fluorescent worms chosen for further investigation. Transgenic worms were maintained by a standard procedure in the lab and then frozen in freezing buffer (100 mM NaCl, 50 mM KPO₄, 30% glycerol, 300 μM MgSO₄) at –80 °C for 24 h then transferred to liquid nitrogen for permanent storage.

In Vivo FRET Measurements on BAECs and C. elegans

Cells transiently expressing the chimeric proteins were observed at room temperature in normal saline (140 mM NaCl; 10 mM HEPES pH 7.3; 5 mM KCl; 2 mM CaCl₂; 0.5 mM MgCl₂; 5 mM glucose) with 63 \times oil immersion Plan-Apochromat objective on both Axio observer A1 and Z1 microscopes (Carl Zeiss). The Z1 microscope was equipped with Definite Focus Z-axis controller and controlled by $\mu\text{Manager}$ v1.3 software (Vale Lab, University of California San Francisco, <http://www.micro-manager.org/index.php>). We used 436 nm excitation (D436/20 filter, Chroma Technology, VT) from a mercury arc lamp controlled by a Lambda 10-2 shutter/filter wheel (Suttter Instruments, CA, USA). Cells were imaged with an iXon DVC887 cooled back-illuminated CCD camera (Andor, CT, USA). Donor and acceptor channels were split by a Dual-View equipped with OI-04-EM 505dxc D465/30m D535/30m splitter (Mag Biosystems). FRET ratio images were calculated as described in the *in vitro* DNA stretching analysis, except that the intensities derived from the microscope are of wider bandwidth. All dynamic studies were corrected for photobleaching by using the rate of bleach in control cells/worms that were not stimulated or treated. Images from trypsin treated BAECs were obtained after 15 min trypsinization at room temperature (2.5% trypsin, 1 mM EDTA in HEPES buffer). Actin disassembly was induced with 30 μM cytochalasin-D and 20 μM latrunculin in normal saline + 2.5% DMSO. Stretching with solution flow over the BAECs was produced with pressure applied to a ~ 4 μm pipette tip placed ~ 10 μm away from the cell. Pressure steps were produced from an HSPC-1 pressure clamp (ALA Scientific Instruments, NY, USA) controlled by pClamp 9.0 software (Molecular Devices, Sunnyvale, CA, USA). Shear force was estimated using fluorescent microspheres imaged at 250 frames/s as they exited the pipette tip, and entering the velocity data into a COMSOL numerical simulations that modeled shear

flow over a surface 20 μm away from a 4 μm exit port. Images were processed using ImageJ (<http://rsb.info.nih.gov/ij>) software and Origin 7.0 was used for data analysis and plotting. Since mechanical stimuli produce spatiotemporal changes to structural elements within a cell, the stressed region will move with time effecting the measurement. To compensate for this motion we developed a plugin for ImageJ called Measure-Track (<http://rsb.info.nih.gov/ij/plugins/measure-track/index.html>) that measures the motion of a fiducial marker in the X - Y plane and applies this motion to a nearby region of interest (ROI). This allows an ROI to track moving objects in video data (courtesy C. Nicolai, SUNYAB).

Caenorhabditis elegans worms expressing stFRET-collagen-19 were grown on Nematode Growth Medium plates.⁵ Worm cuticles were prepared by first sonicating worms 5 times with 20 s bursts in 10 mM Tris pH 7.4, 1 mM EDTA, 1 mM PMSF followed by 2 washes and detergent extraction. Three detergent extraction methods tested included 2.5 h in 1% SDS, 2 h in 1% Triton-X100 and 2 h in 1% NP-40.

Live worms were restrained by grabbing the head and tail with two suction pipettes held in micromanipulators (see Fig. 5c). This allowed us to focus on the stationary end, keeping it in focus while we stretched the worm by pulling the other end.

Statistics

Statistical differences between mean measurements were determined using an independent two sample t test set at the 0.05 significance level. All errors on averaged data are standard errors of the mean.

ELECTRONIC SUPPLEMENTARY MATERIAL

The online version of this article (doi:[10.1007/s12195-010-0140-0](https://doi.org/10.1007/s12195-010-0140-0)) contains supplementary material, which is available to authorized users.

ACKNOWLEDGMENTS

We acknowledge the assistance of the Confocal Microscope and Flow Cytometry Facility in the School of Medicine and Biomedical Sciences, University at Buffalo and support from the NIH.

AUTHOR CONTRIBUTIONS

Fanjie Meng—Designed and constructed stFRET probes, DNA stretching of stFRET, Imaging and analysis of constitutive strain, Wrote paper.

Thomas Suchyna—Designed performed mechanical stimulation experiments, FRET systems calibration/characterization, Imaging and analysis of constitutive strain, Wrote paper.

Elena Lazakovitch—Injected *C. elegans* oocytes and cultured worms, detergent solubilization of worms.

Richard M. Gronostajski—Collagen construct design, worm injection, edited paper.

Frederick Sachs—Project design, data analysis, Wrote paper.

REFERENCES

- ¹An, X., M. C. Lecomte, J. A. Chasis, N. Mohandas, and W. Gratzer. Shear-response of the spectrin dimer-tetramer equilibrium in the red blood cell membrane. *J. Biol. Chem.* 277:31796–31800, 2002.
- ²Avvisato, C. L., *et al.* Mechanical force modulates global gene expression and beta-catenin signaling in colon cancer cells. *J. Cell Sci.* 120:2672–2682, 2007.
- ³Benz, P. M., *et al.* Cytoskeleton assembly at endothelial cell-cell contacts is regulated by alphaII-spectrin-VASP complexes. *J. Cell Biol.* 180:205–219, 2008.
- ⁴Besch, S. R., T. Suchyna, and F. Sachs. High-speed pressure clamp. *Pflugers Arch.-Eur. J. Physiol.* 445:161–166, 2002.
- ⁵Brenner, S. The genetics of *Caenorhabditis elegans*. *Genetics* 77:71–94, 1974.
- ⁶Brown, A. E. X., R. I. Litvinov, D. E. Discher, and J. W. Weisel. Forced unfolding of coiled-coils in fibrinogen by single-molecule AFM. *Biophys. J.* 92:L39–L41, 2007.
- ⁷Carter, N. J., and R. A. Cross. Kinesin's moonwalk. *Curr. Opin. Cell Biol.* 18:61–67, 2006.
- ⁸Croft, D. R., *et al.* Actin-myosin-based contraction is responsible for apoptotic nuclear disintegration. *J. Cell Biol.* 168:245–255, 2005.
- ⁹Cunningham, C. C., *et al.* Actin-binding protein requirement for cortical stability and efficient locomotion. *Science* 255:325–327, 1992.
- ¹⁰Esue, O., Y. Tseng, and D. Wirtz. Alpha-actinin and filamin cooperatively enhance the stiffness of actin filament networks. *PLoS One* 4:e4411, 2009.
- ¹¹Ferrer, J. M., *et al.* Measuring molecular rupture forces between single actin filaments and actin-binding proteins. *Proc. Natl Acad. Sci. USA* 105:9221–9226, 2008.
- ¹²Forde, N. R., D. Izhaky, G. R. Woodcock, G. J. Wuite, and C. Bustamante. Using mechanical force to probe the mechanism of pausing and arrest during continuous elongation by *Escherichia coli* RNA polymerase. *Proc. Natl Acad. Sci. USA* 99:11682–11687, 2002.
- ¹³Furuike, S., T. Ito, and M. Yamazaki. Mechanical unfolding of single filamin A (ABP-280) molecules detected by atomic force microscopy. *FEBS Lett.* 498:72–75, 2001.
- ¹⁴Gardel, M. L., *et al.* Prestressed F-actin networks cross-linked by hinged filamins replicate mechanical properties of cells. *Proc. Natl Acad. Sci. USA* 103:1762–1767, 2006.
- ¹⁵Gosse, C., and V. Croquette. Magnetic tweezers: micro-manipulation and force measurement at the molecular level. *Biophys. J.* 82:3314–3329, 2002.
- ¹⁶Huang, S., and D. E. Ingber. The structural and mechanical complexity of cell-growth control. *Nat. Cell Biol.* 1:E131–E138, 1999.

- ¹⁷Johnson, C. P., H. Y. Tang, C. Carag, D. W. Speicher, and D. E. Discher. Forced unfolding of proteins within cells. *Science* 317:663–666, 2007.
- ¹⁸Kainulainen, T., *et al.* Cell death and mechanoprotection by filamin in connective tissues after challenge by applied tensile forces. *J. Biol. Chem.* 277:21998–22009, 2002.
- ¹⁹Kramer, J. M. Structures and functions of collagens in *Caenorhabditis elegans*. *FASEB J.* 8:329–336, 1994.
- ²⁰Kramer, J. M., J. J. Johnson, R. S. Edgar, C. Basch, and S. Roberts. The *sqt-1* gene of *C. elegans* encodes a collagen critical for organismal morphogenesis. *Cell* 55:555–565, 1988.
- ²¹Lamaze, C., L. M. Fujimoto, H. L. Yin, and S. L. Schmid. The actin cytoskeleton is required for receptor-mediated endocytosis in mammalian cells. *J. Biol. Chem.* 272:20332–20335, 1997.
- ²²Leikina, E., M. V. Merts, N. Kuznetsova, and S. Leikin. Type I collagen is thermally unstable at body temperature. *Proc. Natl Acad. Sci. USA* 99:1314–1318, 2002.
- ²³Liu, L., M. P. Jedrychowski, S. P. Gygi, and P. F. Pilch. Role of insulin-dependent cortical fodrin/spectrin remodeling in glucose transporter 4 translocation in rat adipocytes. *Mol. Biol. Cell* 17:4249–4256, 2006.
- ²⁴MacDonald, R. I., and E. V. Pozharski. Free energies of urea and of thermal unfolding show that two tandem repeats of spectrin are thermodynamically more stable than a single repeat. *Biochemistry* 40:3974–3984, 2001.
- ²⁵Martin, P., and S. M. Parkhurst. Development: may the force be with you. *Science* 300:63–65, 2003.
- ²⁶Matthews, B. D., D. R. Overby, R. Mannix, and D. E. Ingber. Cellular adaptation to mechanical stress: role of integrins, Rho, cytoskeletal tension and mechanosensitive ion channels. *J. Cell Sci.* 119:508–518, 2006.
- ²⁷Mello, C. C., J. M. Kramer, D. Stinchcomb, and V. Ambros. Efficient gene transfer in *C. elegans*: extra-chromosomal maintenance and integration of transforming sequences. *EMBO J.* 10:3959–3970, 1991.
- ²⁸Meng, F., T. M. Suchyna, and F. Sachs. A fluorescence energy transfer-based mechanical stress sensor for specific proteins in situ. *FEBS J.* 275:3072–3087, 2008.
- ²⁹Min, W., *et al.* Fluctuating enzymes: lessons from single-molecule studies. *Acc. Chem. Res.* 38:923–931, 2005.
- ³⁰Myllyharju, J., and K. I. Kivirikko. Collagens, modifying enzymes and their mutations in humans, flies and worms. *Trends Genet.* 20:33–43, 2004.
- ³¹Na, S., *et al.* Rapid signal transduction in living cells is a unique feature of mechanotransduction. *Proc. Natl Acad. Sci. USA* 105:6626–6631, 2008.
- ³²Nagai, T., *et al.* A variant of yellow fluorescent protein with fast and efficient maturation for cell-biological applications. *Nat. Biotechnol.* 20:87–90, 2002.
- ³³Ohta, Y., N. Suzuki, S. Nakamura, J. H. Hartwig, and T. P. Stossel. The small GTPase RalA targets filamin to induce filopodia. *Proc. Natl Acad. Sci. USA* 96:2122–2128, 1999.
- ³⁴Okreglak, V., and D. G. Drubin. Loss of Aip1 reveals a role in maintaining the actin monomer pool and an in vivo oligomer assembly pathway. *J. Cell Biol.* 188:769–777, 2010.
- ³⁵Primalov, P. Physical basis of the stability of folded conformations of proteins. New York: Freeman, 1992.
- ³⁶Qu, H., C. Y. Tseng, Y. Wang, A. J. Levine, and G. Zocchi. The elastic energy of sharply bent nicked DNA. *EPL* 90:1–5, 2010.
- ³⁷Rief, M., J. Pascual, M. Saraste, and H. E. Gaub. Single molecule force spectroscopy of spectrin repeats: low unfolding forces in helix bundles. *J. Mol. Biol.* 286:553–561, 1999.
- ³⁸Rizzo, M. A., G. H. Springer, B. Granada, and D. W. Piston. An improved cyan fluorescent protein variant useful for FRET. *Nat. Biotechnol.* 22:445–449, 2004.
- ³⁹Sarkar, A., S. Caamano, and J. M. Fernandez. The elasticity of individual titin PEVK exons measured by single molecule atomic force microscopy. *J. Biol. Chem.* 280:6261–6264, 2005.
- ⁴⁰Schmoller, K. M., O. Lieleg, and A. R. Bausch. Internal stress in kinetically trapped actin bundle networks. *Soft Matter* 4:2365–2367, 2008.
- ⁴¹Schwaiger, I., C. Sattler, D. R. Hostetter, and M. Rief. The myosin coiled-coil is a truly elastic protein structure. *Nat. Mater.* 1:232–235, 2002.
- ⁴²Schwaiger, I., M. Schleicher, A. A. Noegel, and M. Rief. The folding pathway of a fast-folding immunoglobulin domain revealed by single-molecule mechanical experiments. *EMBO Rep.* 6:46–51, 2005.
- ⁴³Soncini, M., *et al.* Mechanical response and conformational changes of alpha-actinin domains during unfolding: a molecular dynamics study. *Biomech. Model. Mechanobiol.* 6:399–407, 2007.
- ⁴⁴Suchyna, T. M., and F. Sachs. Mechanosensitive channel properties and membrane mechanics in mouse dystrophic myotubes. *J. Physiol.* 581:369–387, 2007.
- ⁴⁵Thein, M. C., *et al.* *Caenorhabditis elegans* exoskeleton collagen COL-19: an adult-specific marker for collagen modification and assembly, and the analysis of organismal morphology. *Dev. Dyn.* 226:523–539, 2003.
- ⁴⁶Trepat, X., *et al.* Universal physical responses to stretch in the living cell. *Nature* 447:592–595, 2007.
- ⁴⁷Wakatsuki, T., B. Schwab, N. C. Thompson, and E. L. Elson. Effects of cytochalasin D and latrunculin B on mechanical properties of cells. *J. Cell Sci.* 114:1025–1036, 2001.
- ⁴⁸Wang, Y., A. Wang, H. Qu, and G. Zocchi. Protein–DNA chimeras: synthesis of two-arm chimeras and non-mechanical effects of the DNA spring. *J. Phys. Condens. Matter* 21:1–11, 2009.
- ⁴⁹Wang, A., and G. Zocchi. Elastic energy driven polymerization. *Biophys. J.* 96:2344–2352, 2009.
- ⁵⁰Wiggins, P. A., *et al.* High flexibility of DNA on short length scales probed by atomic force microscopy. *Nat. Nanotechnol.* 1:137–141, 2006.
- ⁵¹Zhang, Z., S. A. Weed, P. G. Gallagher, and J. S. Morrow. Dynamic molecular modeling of pathogenic mutations in the spectrin self-association domain. *Blood* 98:1645–1653, 2001.